Short Communication

The Electrocatalytic Activity of Polyaniline/TiO$_2$ Nanocomposite for Congo Red Degradation in Aqueous Solutions

Khadija M. Emran[1], Shimaa M. Ali[1,2], Aishah L.L. Al-Oufi[1]*

[1] Department of Chemistry, Faculty of Science, Taibah University, Madinah 30002, KSA
[2] Department of Chemistry, Faculty of Science, Cairo University, Giza 12613, Egypt
[*]E-mail: kabdalsamad@taibahu.edu.sa, dr_shimaaali80@yahoo.com

A nano-composite of polyaniline with TiO$_2$ (PANI/TiO$_2$) is prepared using the chemical oxidative polymerization method. The prepared composite is characterized using x-ray diffraction (XRD), transmission and scanning electron microscopes (TEM and SEM), Fourier transform infrared spectroscopy (FTIR), and thermal analysis. XRD and TEM reveal the formation of the orthorhombic phase of PANI/TiO$_2$ with an average particle size of 8 nm. The FTIR spectrum of the nano-composite shows the presence of characteristic oxide peaks in addition to PANI peaks. Thermal analysis confirms the increased thermal stability of PANI after composite formation. The PANI/TiO$_2$ composite has been used as a catalyst for Congo red degradation using electrochemical oxidation. Several parameters which affect the percent removal are studied such as pH, electrolysis time, applied current density, and initial dye concentration. The optimum conditions for obtaining the highest possible removal efficiency were determined.

1. INTRODUCTION

Water pollution is when any substance is added to the water or when the physical properties of water is changed in a way that impedes its use for its usual purposes [1–4]. One of the most dangerous forms of aqueous pollution is the contamination of water by dyes due to many industries, such as textile, leather, rubber, carpet, etc. [5]. Treatments of dye effluents are difficult and cost ineffective due to their aromatic structures, stability, and non-biodegradability [6]. There are several methods for the removal of dyes from wastewater. These technologies can be divided into three categories: biological, chemical, and physical [7]. In the electrochemical treatment of dye-containing effluents, the organic

dyes are destroyed into non-hazardous products, but the cost of electricity use limits the use of the electrochemical removal [8–12].

Nano-composites are very interesting materials that have attracted researchers for many decades due to their unique properties which allow for their uses in many useful applications [13]. These attractive properties are due to the well and stabilized dispersion of nano-particles. Thus, in polymer/nano-metal oxide composites, metal oxide nano-particles are dispersed in the polymer matrix. In addition, the use of conducting polymers increases the applicability of these materials due to their easy large scale synthesis and multi-functionality [14–19].

Many papers report the electro-oxidation of organic dyes using a variety of nano-oxides as anodes. For example, Wang et al. reported the removal of methylene blue through electrocatalytic degradation using Co doped Ti/TiO_2 nanotube/PbO_2 prepared by a pulse electro-deposition technique [20]. The electrochemical degradation process was studied using steady-state polarization curves, cyclic voltammetry (CV), and electrochemical impendence spectroscopy (EIS). The CV curve in 30 $mg·L^{-1}$ MB in 0.2 $mol·L^{-1}$ Na_2SO_4 showed a clear oxidation peak at 1.43 V. The effect of pH, current density, and initial concentration of methylene blue on the degradation of dyes has been examined. The removal efficiency decreased with increasing the dye concentration. Results indicated that removal efficiency reached 74.0% with a current density of 50 $mA·cm^{-2}$ after 120 min at a pH of 3. The electrochemical degradation of acid blue 113 dye was studied by Moura et al. using three different anodes: platinum supported on Ti (Ti/Pt), lead dioxide (Pb/PbO_2), and TiO_2-nanotubes decorated with PbO_2 supported on Ti (Ti/TiO_2-nanotubes/PbO_2) [21]. Different current density values of 20, 40, and 60 $mA·cm^{-2}$ were investigated. The degradation of dyes was monitored by the UV-visible spectrometry and carbon oxygen demand (COD). The maximum removal efficiency and COD were 98% and 88.4%, respectively. Results showed that acid blue 113 was successfully degraded by hydroxyl radicals electrogenerated from water discharge on the Ti/TiO_2-Nanotubes/PbO_2 electrode surface. The Ti/TiO_2-Nanotubes/PbO_2 anode showed a better performance in removing the acid blue 113 than Ti/Pt and Pb/PbO_2.

In this work, a $PANI/TiO_2$ nanocomposite, prepared by chemical polymerization in the presence of suspended oxide nano-particles, will be employed as an electrocatalyst for the oxidation of Congo red (CR) dye from aqueous solutions. Parameters affecting the electro-degradation process, such as pH, applied current density, electrolysis time, and initial dye concentration, will be optimized.

2. EXPERIMENTAL

2.1 Chemicals

Titan(IV) butoxide (97%), sodium hydroxide (99%), nitric acid (69%), sulfuric acid (95–97%), sodium chloride (99%), aniline (99.5%), and hexadecyltrimethyl-ammomium bromide (CTAB) are purchased from Sigma Aldrich. Congo red ($C_{32}H_{22}N_6Na_2O_6S_2$) was bought from Brixworth (Northants, UK). All solutions are prepared using double distilled water.

2.2 Preparation of Nano-TiO$_2$ and PANI/TiO$_2$ Nanocomposite

Nano-TiO$_2$ can be prepared using the sol–gel method via the hydrolysis of titan(IV) butoxide. The dried gel is calcinated at 350 °C for 2 h [22].

The PANI/TiO$_2$ nanocomposite is prepared by the chemical oxidative polymerization of aniline in the presence of nano-TiO$_2$. Nano-oxide particles are dispersed in 10^{-3} mol·L^{-1} of the surfactant solution, CTAB. Then, an aqueous FeCl$_3$ solution is added while stirring aniline solution in 0.1 mol·L^{-1} H$_2$SO$_4$ is injected into the solution drop by drop. Nano-composite is filtered, washed, and dried at 80 °C.

2.3 Characterizations of PANI/TiO2 Nanocomposite

X-ray diffraction (XRD) is carried out by x-ray diffractograms (Shimadzu, XRD-7000, Japan) at 40 kV and 30 mA, using a CuK$_\alpha$ incident beam ($\lambda = 0.154$ nm).

The morphology is examined using scanning electron microscopy (Superscan SS-550, Shimadzu, Japan) and transmission electron microscopy (JEOL JEM 1400, Japan).

Samples are recorded on Fourier transform infrared spectroscopy (FTIR) IR Affinity-1S, Shimadzu, Japan). Thermal analysis of preheated samples is performed by a Q600 TA Instrument at a heating rate of 10 °C/min from 200 °C to 900 °C.

The remaining concentration of CR, measured at λ_{max} of 498 nm, is determined by a UV-VIS spectrophotometer (Evolution 300 UV-VIS, Thermo Scientific, Germany). The percent removal of the dye can be calculated according to

$$\text{Removal} \% = \frac{C_0 - Ce}{C_0} \times 100$$

where C$_0$ and C$_e$ are initial and equilibrium dye concentrations (mg·L^{-1}), respectively.

COD is measured using a COD reactor and a spectrophotometer (DR/5000, Hach, USA). The COD percent removal is calculated using the following formula

$$\text{Removal} \% = \frac{COD_0 - COD_t}{COD_0} \times 100$$

where COD$_0$ is the COD of the initial concentration and COD$_t$ is the COD at a given time (t).

2.4 Dye Removal by Electro-Oxidation

A graphite disc electrode (d = 0.5 cm) is used as a support for a PANI/TiO$_2$ composite and acts as an anode while a parallel steel rod (d = 0.6, L = 2 cm) acts as the cathode. These electrodes are separated from each other by a constant distance of 20 mm, connected to a 5 A, 10 V DC power supply, and placed in an 80 mL NaCl solution as a supporting electrolyte. The solution was kept under agitation using a magnetic stirrer for 30 min.

3. RESULTS AND DISCUSSION

3.1 Structural, Surface, and Thermal Characterizations of the PANI/TiO$_2$ Nanocomposite
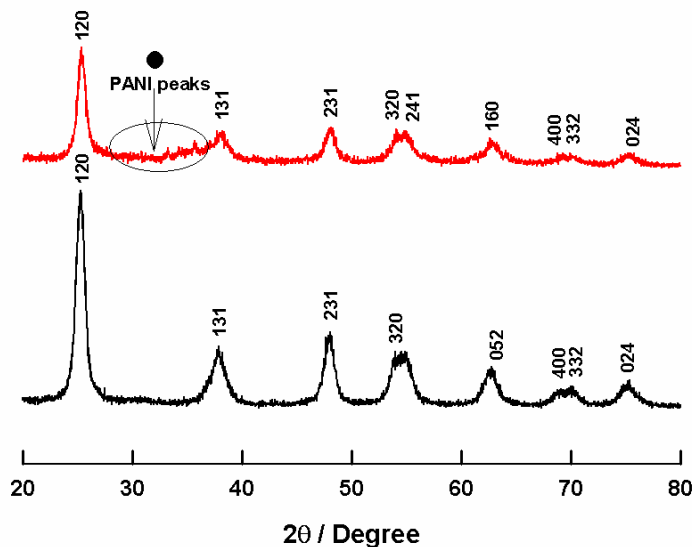
Figure 1. XRD patterns of TiO$_2$ (black line) and its composite with PANI (red line). Miller indices are indicated for TiO$_2$ peaks.

Table 1. Structural parameters, calculated from XRD data, for TiO$_2$ and PANI/TiO$_2$ composites and BET surface area values.

Sample	Geometry	Lattice parameter Å	Lattice volume Å^3	Density g cm^{-3}	BET m^2 g^{-1}
TiO$_2$/Standard	Orthorhombic	a=5.46 b=9.18 c=5.14	257.63	4.12	-
TiO$_2$/Sample	Orthorhombic	a=5.44 b=9.22 c=4.98	249.74	4.52	132.28
PANI/TiO$_2$/Sample	Orthorhombic	a=5.42 b=9.19 c=5.21	259.70	4.04	96.13

Figure 1 shows XRD patterns of nano-TiO$_2$ (black line) and its composite with PANI (red line). Diffraction peaks are compared with the Joint Committee on Powder Diffraction Standards, JCPDS card of TiO$_2$ (card number 00-015-0875). Results confirm the formation of the pure orthorhombic phase of TiO$_2$ which has a crystalline structure. Therefore, PANI peaks cannot be observed. The oxide structure is not affected by forming a composite with PANI**.** Characteristic peaks of PANI at 2θ = 25–35° [23,24] cannot be observed clearly due to the amorphous nature of the polymer. The average

particle size can be calculated using Debye–Scherrer's equation [25]. The calculated particle size values are 6.5 and 8.1 nm for TiO_2 and its composite with PANI, respectively. Structural parameters such as the lattice parameter, lattice volume, and theoretical density are calculated from XRD data and listed in Table 1. Good agreement is observed with those values in the ICDD card. The BET surface area values are 132.28 and 96.13 $m^2 \cdot g^{-1}$ for TiO_2 and the $PANI/TiO_2$ composite, respectively. The decreased surface area of the composite with respect to the oxide can be due to the increased particle size of the composite having the core-shell structure where the nano-oxide particle acts as a nucleus for polymer growth.
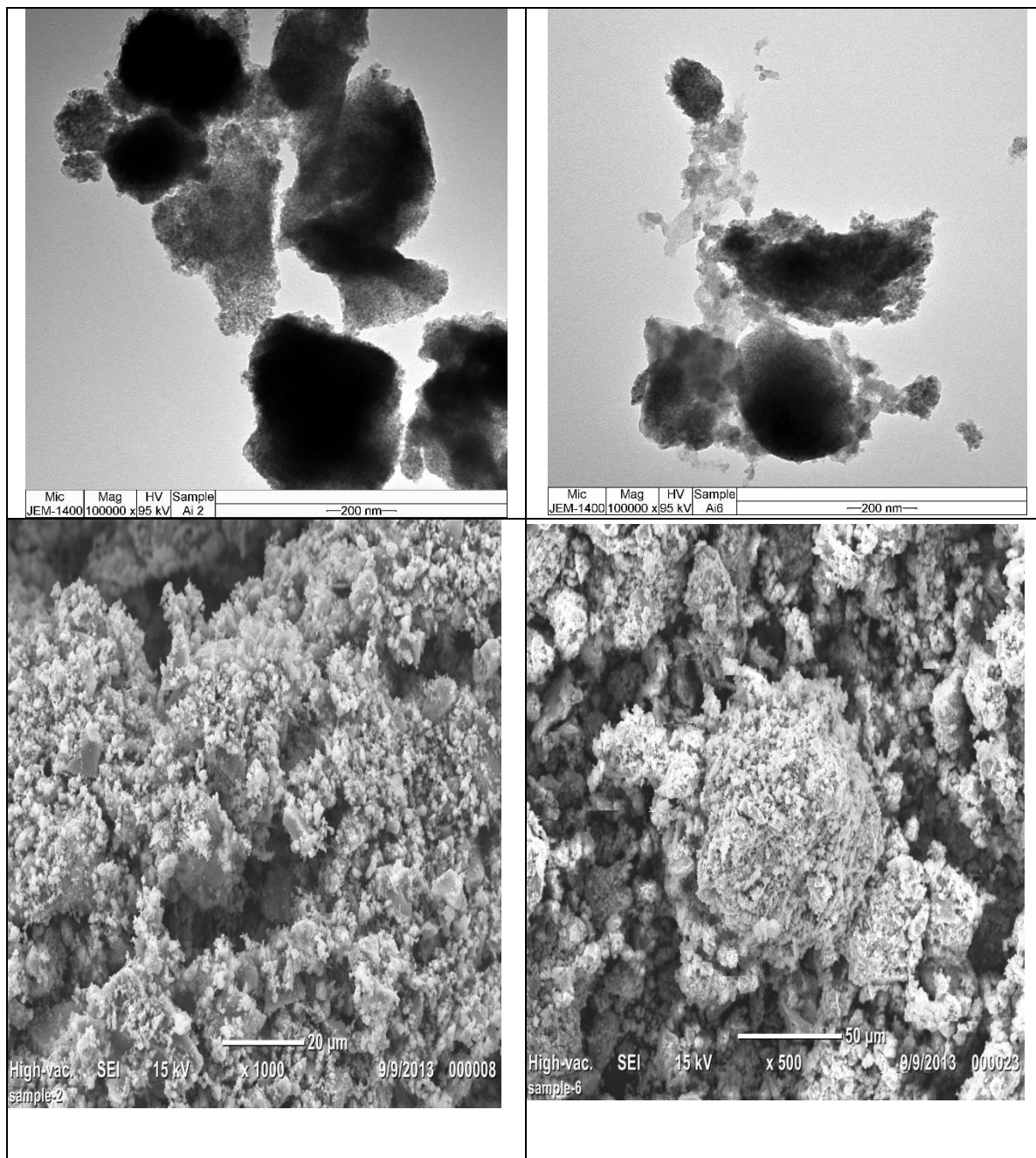
Figure 2. (**a, b**) TEM and (**a', b'**) images of TiO_2 and $PANI/TiO_2$ composite, respectively.

Figure 2 shows TEM images of the (a) TiO_2 and (b) PANI/TiO_2 composite. The orthorhombic phase can be clearly observed for TiO_2 oxide and its composite with PANI. The calculated average particle size values are 6.5 and 7.9 nm, respectively. These results are comparable with those obtained by XRD analysis. Figure 2 shows SEM photos of the (a') TiO_2 and (b') PANI/TiO_2 composite. Orthorhombic grains are seen for the oxide while an amorphous and rough surface is characteristic for the PANI/TiO_2 composite. From energy dispersive X-rays (EDX) analysis, the nitrogen percentage in the composite is 3.6%, confirming the presence of PANI in the composite.

The FTIR spectra for the PANI and PANI/TiO_2 composite are showed by Figure 3. Standard FTIR peaks for PANI appear at 1582 and 1120 cm^{-1} which indicate quinone ring absorption. Peaks located at 1289 cm^{-1} correspond to C–N stretching, and peaks at 1492 and 801 cm^{-1} indicate benzene ring absorption [26]. On the other hand, the FTIR spectrum for the nano-composite shows an additional peak of the TiO vibration band at 507 cm^{-1} [27].
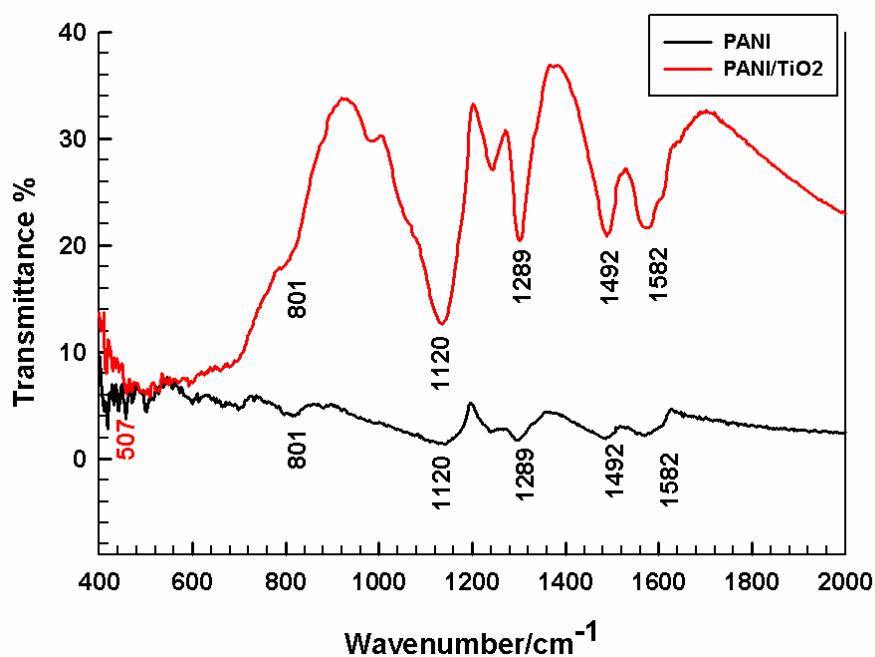
Figure 3. FTIR spectra of the PANI and PANI/TiO_2 composite.

The thermal gravimetric analysis (TGA) curve for PANI and its nano-composite are presented by Figure 4. It is well known that TiO_2 is thermally stable over the studied temperature range [28]. On the other hand, PANI decomposes sharply at 404 °C (Figure 4). On examining TGA curves, it can be observed that the PANI nano-composite has higher thermal stability than pure PANI, as indicated by the decreased weight loss, reflecting its applicability for use at elevated temperatures. The percentage of PANI in the composite can be calculated by comparing weight loss at the degradation temperature of PANI for both PANI and PANI/TiO_2 samples. It is found that 12% of the composite consists of PANI, suggesting a thin shell polymer/core nano-oxide structure.
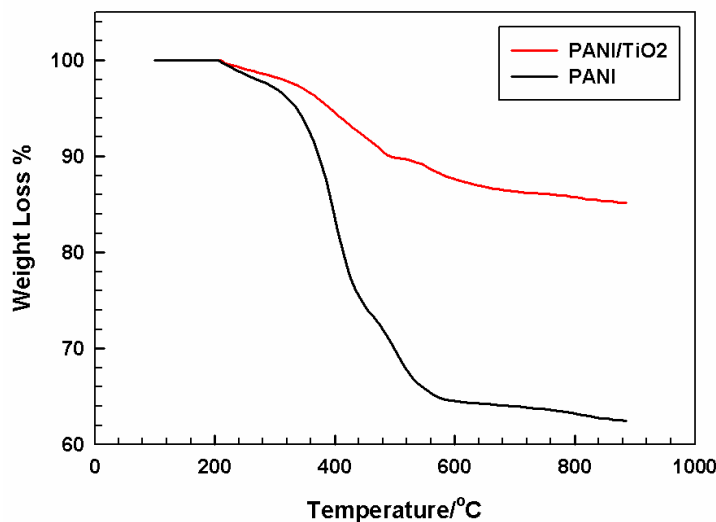
Figure 4. TGA curves of PANI and PANI/TiO$_2$ composites at a heating rate of 10 °C min^{-1} under a nitrogen atmosphere.

3.2 Removal of Organic Dye Pollutants Using PANI/TiO2 Nanocomposite via Electro-Oxidation

In this section, it will be discussed how CR dye will be removed from aqueous solutions by using a PANI/TiO$_2$ nanocomposite as an electrocatalyst for electro-oxidation. Several parameters affecting the percent removal, such as pH, electrolysis time, applied current density, and initial dye concentration, will be investigated.

3.2.1 pH and Electrolysis Time Effects

The electrochemical degradation of CR by the electro-oxidation on the PANI/TiO$_2$ nano-composite has been studied in the pH range from 4 to 10. The electrolysis is carried out by applying a current density of 1.7647 A·m^{-2} for an initial dye concentration of 200 mg L^{-1} at room temperature. Figure 5 shows the variation of percentage of dye removal with the electrolysis time at different pH values of CR solution. The percent removal increases with time; the maximum percent removal of CR dye is obtained at an electrolysis time of 30 min. At a further electrolysis time, there is no predominant enhancement in the percent removal value. Moreover, the percent removal for CR dye is high and close to 100% in acidic and neutral media, while it sharply decreased in basic media. This can be explained because, in the acidic solution, chloride ions are reduced to chlorine. The latter is a well-known oxidizing agent which facilitates dye degradation by oxidation [29–32]. On the other hand, the presence of chlorate/perchlorate ions (at the expense of chlorine formation) is the key reason for the decreased percent removal in an alkaline medium.
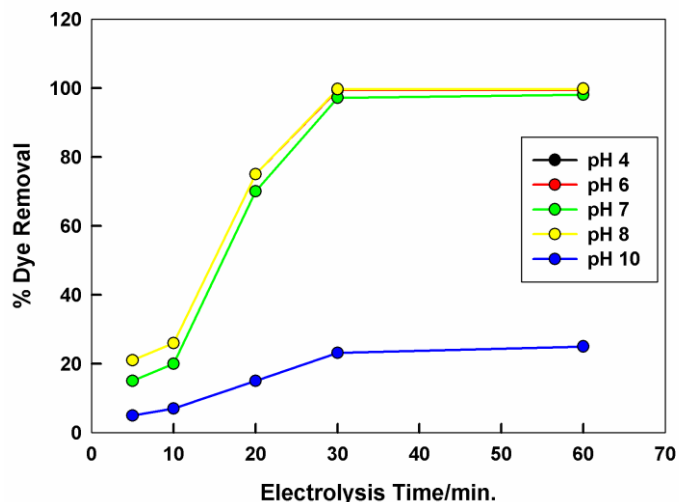
Figure 5. The variation in the percent removal of CR dye with electrolysis time at different pH values of dye solution, dye concentration of 200 mg·L^{-1}, and a current density of 1.7647 A·m^{-2}.

3.2.2 Effect of the Applied Current Density

Different current densities were applied to the graphite electrode coated with PANI/TiO$_2$ composite to investigate the influence of current density on the electrochemical degradation of CR at an initial dye concentration of 200 mg·L^{-1}, under a neutral condition (pH = 7) and in room temperature. Figure 6 shows the variation of the percent removal for CR with the electrolysis time at different applied current density values. It can be shown that the percent removal increased when increasing the applied current density. Because the formation of oxidants such as chlorine/hypochlorite and hydroxyl radicals is facilitated by higher current densities [29]. It can be noticed that, at higher current densities ($>$1.7647 A·m^{-2}), the degradation percent attained an almost constant value.
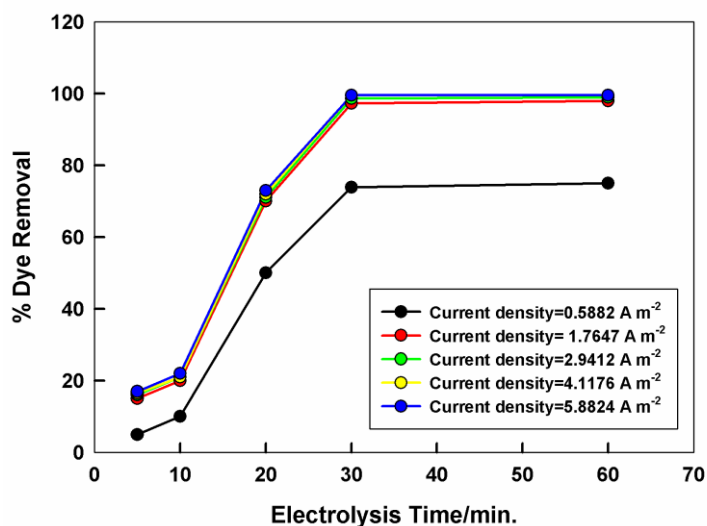
Figure 6. The variation of the percent removal of CR dye and the electrolysis time at different applied current densities in a pH of 7 and a dye concentration of 200 mg·L^{-1}.

3.2.3 Effect of the Initial Dye Concentration
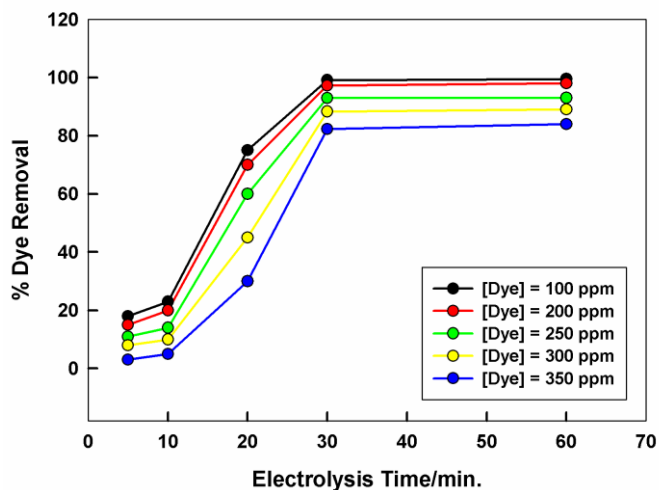
Figure 7. The variation of the percent removal of CR dye and the electrolysis time at different initial dye concentrations, in a pH of 7, and under an applied current density of 1.7647 A·m^{-2}.

Figure 7 shows the variation of the degradation rate expressed as the percent removal of CR dye with the electrolysis time at different initial dye concentrations. There is a decrease in the percent removal with increasing initial dye concentrations. This is due to the increased number of intermediates produced at higher dye concentrations which compete with the adsorption and/or the electro-oxidation of CR at the anode surface and, thus, affect the percent removal [20]. However, this decrease in the percent removal value is not significant. It decreased from 98 to 80% after increasing CR concentrations from 100 to 350 mg·L^{-1} at the optimum electrolysis time of 30 min. This is considered as an advantage to the presented nano-PANI/TiO$_2$ electrocatalyst.

In addition to absorbance data, the percentage of dye removal has also been calculated from COD data at different parameters affecting the electro-oxidation process. Table 2 summarizes the values of the percent removal at different pH values of CR solution, electrolysis times, applied current densities, and initial dye concentrations in terms of both absorbance and COD data. It is clearly shown that there is excellent agreement between the percent removal values calculated from both sets of data. Again, equilibrium is attained at an electrolysis time of 30 min. The percent removal is high under acidic and neutral conditions and decreased in alkaline medium. The percent removal increases until an applied current density of 1.7647 A·m^{-2} is reached. After this value, there is no obvious increase in the percent removal value. The increase in the initial dye concentration results in a decrease in the percent removal values. It is worth mentioning that, while changing a parameter and calculating the percent removal, optimum values of other affecting parameters are adjusted. The optimum conditions for the electro-oxidation of CR dye on the PANI/TiO2 nanocomposite are a pH of 7, electrolysis time of 30 min, applied current density of 1.7647 A·m^{-2}, and an initial dye concentration of 200 mg·L^{-1}.

Table 2. Comparison between the percent removal values calculated from absorbance and COD data at different parameters.

pH Value	4	6	7	8	10
%Removal, Absorbance	99.39	99.70	97.23	99.70	23.14
%Removal, COD	96.87	97.63	96.66	97.14	25.25
Electrolysis Time, min	5	10	20	30	60
%Removal, Absorbance	19.33	24.73	73.48	97.23	99.62
%Removal, COD	17.37	25.23	75.53	96.66	98.25
Applied current density, A m^{-2}	0.5882	1.7647	2.9412	4.1176	5.8824
%Removal, Absorbance	73.85	97.23	98.65	99.51	99.49
%Removal, COD	72.53	96.66	97.29	97.25	97.41
Initial dye conc., mg L^{-1}	100	200	250	300	350
%Removal, Absorbance	99.11	97.23	92.91	88.31	82.32
%Removal, COD	98.29	96.66	92.76	87.92	80.94

4. CONCLUSIONS

- PANI/TiO$_2$ nanocomposite is successively prepared by the chemical oxidation of the monomer in the suspended oxide solution.
- XRD and TEM confirm the formation of the nano-composite with an orthorhombic structure and average particle size of 8 nm. SEM images show that the surface roughness and compactness of nano-oxide increases by forming a composite with PANI.
- The removal of CR by the electro-oxidation, using PANI/TiO$_2$ composite as an anode, has been done successfully in aqueous solutions.
- Critical parameters affecting the electro-oxidation process such as pH, applied current density, electrolysis time, and initial dye concentration are optimized. The best conditions that result in the highest percent removal are a pH of 7, an electrolysis time of 30 min, and a current density 1.7647 of A·m^{-2}.

References

1. F.Greenlee, D. Lawler, B. Freeman, B. Marrot, P. Moulin, *Water Res.*, 43(2009)2317.

2. M. Khehra, H. Saini, D. Sharma, B. Chadha, S. Chimni, *Dye. Pigment.,* 70(2006)1.
3. S.Dawood, T. Sen, *J. Chem. Proc. Eng.* 1 (2014)11.
4. S. Chatterjee, D. Lee, M. Lee, S., Woo, *Bioresour. Technol.*, *100* (2009)2803.
5. R. Gong, Y. Ding, M. Li, C. Yang, H. Liu, Y. Sun, *Dye. Pigment.*, 64(2005)187.
6. Y.Pang, A. Abdullah, *Water*, 41 (2013)751.
7. T. Robinson, G. Mcmullan, R. Marchant, P. Nigam, *Bioresour. Technol.*, 77(2001) 247.
8. A. Charoensri, F. Kobayashi, A. Kimura, J. Ishii, *J. Met. Mater. Miner.*, 16(2006)57.
9. R. Saratale, G. Saratale, J. Chang, S. Govindwar, *J. Taiwan Inst. Chem. Eng.* , 42(2011)138.
10. L. Chingi, J. Changi, T. Wen, *Water Res.,* 29(1994)671.
11. J. Parsa, M. Abbasi, *Acta Chim. Slov.,* 54 (2007)792.
12. A. Maljaei, M. Arami, N. Mahmoodi, *Desalination*, 249(2009)1074.
13. W. Miled, A. Said, S. Roudesli, *J. Text. Apparel, Technol. Manag.,* 6(2010)1.
14. T. Alemayehu, B. Himariam, *Int. J. Recent Res. Phys. Chem. Sci.*, 1(2014) 24.
15. L. Mobarakeh, M. Prabhakaran, M. Morshed, H. Esfahani, M.Baharvand, S. Kiani, S. Al-Deyab, S. Ramakrishna, *J. Tissue Eng. Regen. M.*,5(2011)17.
16. A. Macdiarmid, J. Chiang, *Synth. Met.*, 18(1987) 285.
17. A. Michaels, H. Bixler, *J. Polym. Sci.*, 50(1961) 393.
18. M. Harun, E. Saion, A. Kassim, N.Yahya, E. Mahmud, *J. Adv. Sci. Arts*, 2 (2007)63.
19. L.Zhang, M. Fang, *Nano Today, 5*(2010)128.
20. C. Wang, F.Wang, M. Xu, C.Zhu, W.Fang, Y. Wei, *J. Electroanal. Chem.*, 759 (2015)158.
21. D. De Moura, M. Quiroz, D.Da Silva, R. Salazar, C.Martínez-Huitle, *Environ. Nanotechnology, Monit. Manag.*, 5(2016)13.
22. B. Li, X.Wang, M.Yan, L. Li, *Mater. Chem. Phys.*, 78(2002)184.
23. A.Rahy, D. Yang, *Mater. Lett.* 62 (2008)4311.
24. F.Wei, S.Enhai, F.Akihiko, W. Hongcai, N.Koichi, Y. Katsumi, *Bull. Chem. Soc. Jpn*., 73(2000)2627.
25. Cullity, B. Elements of X-ray diffraction; addision Wealey : New York, 1978.
26. M. Khairy, *J. Alloys Compd.*, 608(2014)283.
27. M. Hamza, F. Saiof, A. Al-ithawi, *Adv. Mater. Phys. Chem.*, 2(2013)432.
28. A.Sharma, R.Karn, S.Pandiyan, *J. Basic Appl. Eng. Res.*, 1(2014)1.
29. N. Ghalwa, *Iran. Chem. Soc.*, 2(2005)238.
30. H.Ma, B.Wang, X. Luo, *J. Hazard. Mater.*, 149(2007)492.
31. A.Vlyssides, M.Loizidou, P.Karlis, A.Zorpas, D. Papaioannou, *J. Hazard. Mater.*, 70(1999) 41.
32. E.Chatzisymeon, N. Xekoukoulotakis, A.Coz, N.Kalogerakis, D.Mantzavinos, *J. Hazard. Mater.*, 137(2006)998.